Energy Dependence of Dispersive effects in Unpolarized Inclusive Elastic Electron/Positron-Nucleus Scattering (PAC53)

Paul Guèye*†, Mark Ddamulira, and Paula Plazas Isanoa

Facility for Rare Isotope Beams Michigan State University, 640 South Shaw Lane East Lansing Michigan 48824, USA

John Arrington*

Lawrence Berkeley National Laboratory, 1 Cyclotron Road Berkeley California 94720, USA

Andrei Afanasev* and Volodymyr Tereshchuk

The George Washington University, 1918 F Street NW Washington District of Columbia 20052, USA

Douglas Highinbotham and Dave Mack

Thomas Jefferson National Accelerator Facility, 12000 Jefferson Avenue Newport News Virginia 23606, USA

Zoë Cogan

The Potter School, East Lansing Michigan, USA

A Jefferson Lab Positron Working Group Proposal

*: Co-spokesperson, †: Contact-spokesperson (gueye@frib.msu.edu)

Executive Summary

Measurements of elastic electron scattering data within the past decade have highlighted two-photon exchange contributions as a necessary ingredient in theoretical calculations to precisely evaluate both inclusive and exclusive elastic cross sections. This correction can modify the cross section at the few percent level. In contrast, dispersive effects that originate from virtual excitation during the scattering process can cause significantly larger deviations. A recent analysis of the ^{12}C electron elastic cross section around the first diffraction minimum, where the Born term contributions to the cross section are small to maximize the sensitivity to dispersive effects, indicates a possible 30% contribution of such effects to the cross section at 1 GeV: their magnitude has been confirmed to be large with a strong energy dependence. Furthermore, the sign of these effects seem to change with the probe, positive (negative) for electrons (positrons), in contradiction with theoretical prediction. These effects could account for a large fraction of the magnitude for the observed quenching of the longitudinal nuclear response (e.g., Coulomb sum rule), play an important role in the extraction of nuclear radii extracted from both unpolarized and parity-violating asymmetry experiments (e.g., neutron skin puzzle), provide constraints on the understanding of the nuclear structure in addition to placing upper limits on the electron dipole moment. **The absolute quantification of these effects require the comparison of elastically scattered electron and positron beams off nuclei**. This proposal aims to map out the magnitude of dispersive effects, e.g., measure both their real and imaginary parts that enter into the scattering amplitude, through unpolarized inclusive $\mathrm{A}(\mathrm{e},\mathrm{e}')$ electron and positron elastic scattering around the first and second diffraction minima of eight nuclei (^{12}C, ^{27}Al, ^{63}Cu, ^{48}Ca, ^{56}Fe, ^{196}Pt, ^{208}Pb and ^{209}Bi) for four incident beam energies (0.70, 1.06, 2.12, and 4.24 GeV) in the experimental Hall C at Jefferson Lab. We propose to accomplish this in two phases: phase 1 will provide qualitative information about these effects from $\mathrm{A}(\mathrm{e}^-,\mathrm{e}^-)$ by comparing the measured cross sections to theoretical calculations and phase 2 will measure the absolute magnitude of these effects by comparing the cross sections from $\mathrm{A}(\mathrm{e}^-,\mathrm{e}^-)$ and $\mathrm{A}(\mathrm{e}^+,\mathrm{e}^+)$. **These measurements will consist of the first ever comprehensive study and energy dependence of these effects.**

Contents

1 Introduction

During the 80s and 90s, higher order corrections to the first Born approximation were extensively studied through dedicated elastic and quasi-elastic scattering experiments using unpolarized electron and positron beams (see [1, 2, 3, 4, 5, 6] and references therein), following the seminal paper from [7]. These effects scale as $S_{HOB} = V_C/E_e$ where S_{HOB} is the scaling factor to account for higher order corrections to the Born approximation, V_C is the Coulomb potential of the target nucleus and E_e is the incident energy of the lepton probe [6]. Incidentally, they are expected to be small in the medium to intermediate energy regime, and have been neglected in the analysis of GeV energy regime.

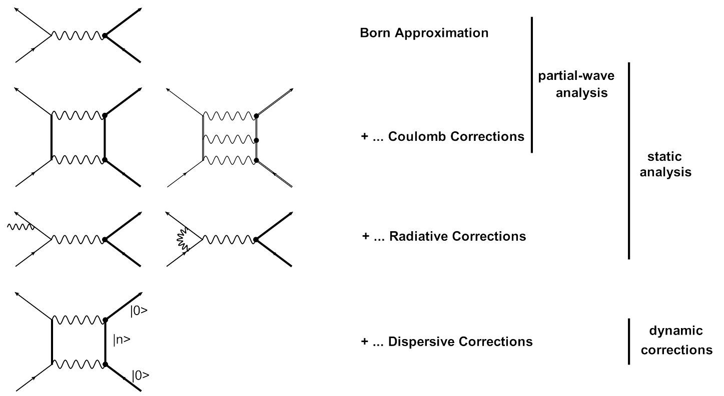

Figure 1: High-order corrections to the one-photon exchange Born approximation in electron/positron-nucleus scattering.

In the 1st order approximation, the scattering cross section is evaluated using plane wave functions for the incoming and outgoing electrons. This approach is also known as the Plane Wave Born approximation (PWBA) or simply the Born Approximation (Fig. 1). Coulomb corrections originate from the Coulomb field of the target nucleus that causes an acceleration (deceleration) of the incoming (outgoing) electrons and a Coulomb distortion of the plane waves: these effects are treated within a Distorted Wave Born Approximation (DWBA) analysis for inelastic scattering or elastic/quasi-elastic scattering on heavy nuclei [6]. Two other corrections are required to properly evaluate the scattering cross section: radiative corrections due to energy loss processes and dispersive effects due to virtual excitations of the nucleus at the moment of the interaction.

Within the last decade, a renewed interest arose from a discrepancy between unpolarized and polarized elastic scattering data on the measurement of the proton form factor ratio $\mu G_E^p/G_M^p$ which can be attributed to the contribution of two-photon exchanges [8, 9, 10, 11, 12, 13, 14, 15]. These effects have been investigated with a series of dedicated experiments [16, 17, 18, 19] (also see reviews [20, 21, 22] and references therein), including their impact on the measurement of form factors for nucleons and light ($A \leq 3$) nuclei. They include both Coulomb corrections [6, 23], excited intermediate states and treatment of the off-shell nucleons through dispersion relations as a function of the 4-momentum transfer.

2 Physics Motivation

2.1 Dispersive Corrections

The electromagnetic nuclear elastic cross section for electrons/positrons can be expressed as:

$$\frac{d\sigma}{d\Omega} = \left(\frac{d\sigma}{d\Omega}\right)_{Mott} \mid F(q^2) \mid^2 \tag{1}$$

where $\left(\frac{d\sigma}{d\Omega}\right)_{Mott}$ is the Mott cross section corresponding to the scattering on a point-like nuclear target, $F(q^2)$ represents the form factor and $q^2 = -Q^2$ is the 4-momentum transfer.

Theoretical calculations for dispersive effects in elastic electron scattering for p-shell, spin-0 targets such as ^{12}C were performed in the mid-70s by Friar and Rosen [24]. They used a harmonic oscillator model and only the longitudinal (Coulomb) component to calculate the scattering amplitude within the PWBA approximation; the transverse component was neglected. The mscattering amplitude – considering only the contribution from the dominant two photon exchange diagrams – can be written as:

$$\mathcal{M}_{disp} = \sum_{n\neq 0} \int \frac{d^3\vec{p}}{\vec{q}_1^2\vec{q}_2^2} \frac{\langle 0|\rho(\vec{q}_2)|n\rangle \langle n|\rho(\vec{q}_1)|0\rangle}{p^2 - p_n^2 - i\varepsilon} a(p_n) \tag{2}$$

with:

$$\begin{cases} a(p_n) &= E_e p_n[1+\cos\theta] + \vec{p}\cdot(\vec{p_e}+\vec{p}_{e'}) \\ p_n &= E_e - \omega_n - \frac{p^2-E_e^2}{2M_p} \\ p &= p_e - p_{e'} \end{cases} \tag{3}$$

where: $p_e = (E_e, \vec{p}_e)$ and $p_{e'} = (E_{e'}, \vec{p}_{e'})$ the 4-momentum of the incoming and outgoing electrons, respectively, and $\vec{q}_{1,2}$ the 3-momenta of the two photons exchanged. θ is the angle between the incoming and outgoing electrons. $\rho(\vec{q}_1)$ and $\rho(\vec{q}_2)$ are the charge operators associated with the two virtual photons, respectively, and using the notation of [24] with $\hat{e}_i(\vec{q})$ the charge distribution (operator in the isospin space) of the i^{th} nucleon, gives:

$$\begin{cases} \rho(\vec{q}) &= \sum_{i=1}^{A} \hat{e}_i(\vec{q}) e^{i\vec{q}\cdot\vec{x}'_i} \\ \hat{e}(\vec{q}) &= \int \hat{e}(\vec{x}) e^{i\vec{q}\cdot\vec{x}} d^3\vec{x} \end{cases} \tag{4}$$

In their calculation, Friar and Rosen [24] also considered that all nuclear excitation states $|n\rangle$ have the same mean excitation energy ω, allowing to apply the closure relation: $\sum |n\rangle\langle n| = 1$. Including the elastic scattering and dispersion corrections leads to:

$$\mathcal{M}_{elast+disp} = (\alpha Z)F(q^2) + (\alpha Z)^2 G(q^2) \tag{5}$$

with $G(q^2)$ arising from two-photon exchange diagrams (including cross-diagram, seagull ...). Hence:

$$\begin{aligned} |\mathcal{M}_{elast+disp}|^2 &= (\alpha Z)^2\big[F(q^2)\big]^2 \\ &+ 2(\alpha Z)^3\big[F(q^2)\mathcal{R}e\{G(q^2)\}\big] \\ &+ (\alpha Z)^4\big[|\mathcal{R}e\{G(q^2)\}|^2 + |\mathcal{I}m\{G(q^2)\}|^2\big] \end{aligned} \tag{6}$$

Therefore, the scattering amplitude is governed by $F(q^2)$ and the real part of $G(q^2)$ outside the minima of diffraction (where $F(q^2) \neq 0$). The imaginary part of $G(q^2)$ is most important inside the minima of diffraction where the term $F(q^2)$ goes to zero.

Experimentally, in order to extract the magnitude of the dispersive effects, one must compare the scattering of both electrons and positrons off nuclear targets to extract $\mathcal{R}e\{G(q^2)\}$ since the even powers in the scattering amplitude cancel. $\mathcal{I}m\{G(q^2)\}$ can then be inferred from the remaining strength observed outside the minima.

The momentum transfer q is also modified to account for the Coulomb effects into an effective momentum transfer q_{eff} [6, 23, 25]:

$$q = 4E_e E_{e'} \sin^2(\theta/2) \rightarrow q_{eff} = 4E_{e,eff} E_{e',eff} \sin^2(\theta/2) \tag{7}$$

with $E_{e,eff} = E_e\left(1 \pm \frac{|V_C|}{E_e}\right)$ and $E_{e',eff} = E_{e'}\left(1 \pm \frac{|V_C|}{E_e}\right)$. $|V_C|$ is the (magnitude of the) Coulomb potential of the target nucleus and the positive (negative) sign accounts for the acceleration (deceleration) of the lepton probe. The corresponding experimentally measured cross section can then be compared to the theoretical cross section calculated using a static charge density [4].

Figure 2 compares the current world data status on the magnitude of dispersive effects in the first minimum of ^{12}C. σ_{stat} represents the cross section obtained from a static charge distribution. The average of a first (solid line) and second (dashed line) order polynomial fits predicts a deviation at

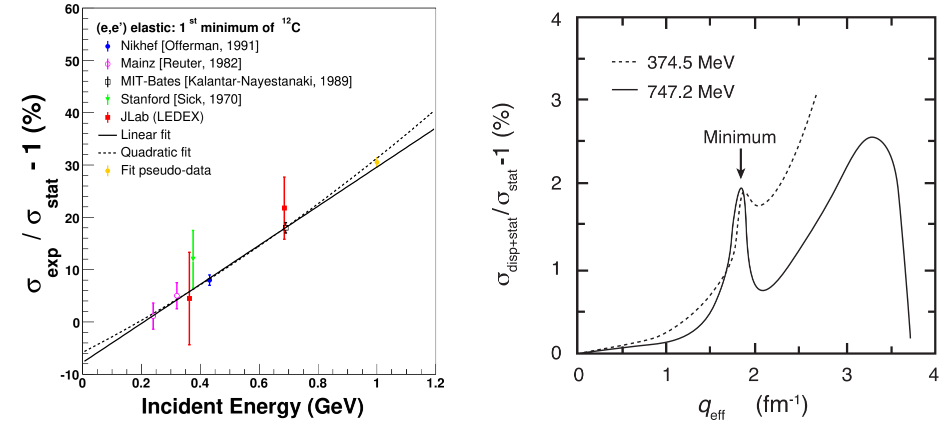

Figure 2: Left panel – World data on the energy dependence of dispersive effects in the first diffraction minimum of ^{12}C. Right panel – Calculations of Friar and Rosen [24] for dispersion corrections to elastic electron scattering from ^{12}C at 374.5 and 747.2 MeV in the first diffraction minimum $q_{eff} = 1.84$ fm^{-1}.

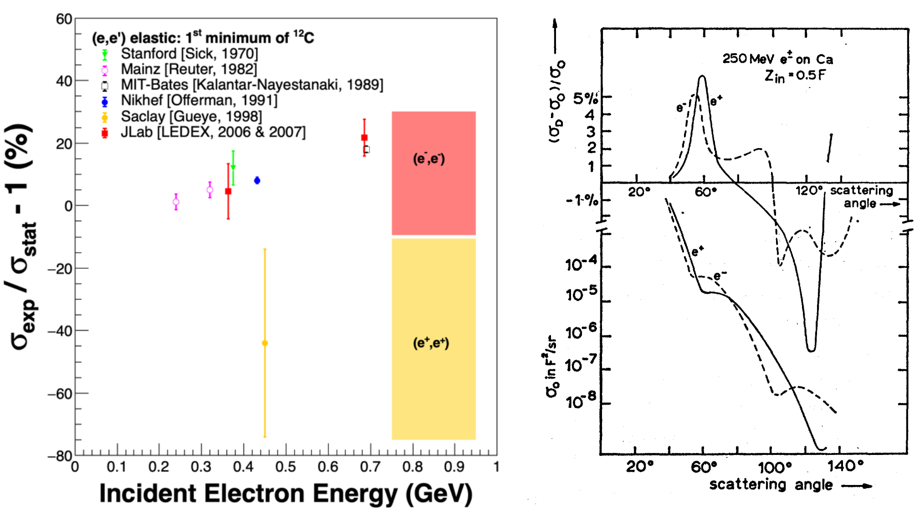

Figure 3: Left panel: dispersive effects measured with a positron beam at 450 MeV compared to electron data in the first minium of diffraction of ^{12}C [5]. Right panel: prediction from Rawitscher [26] showing the dispersion correction for both electrons and positrons on ^{40}Ca at 250 MeV (top) and the location of the first and secon minimum (bottom).

1 GeV of 30.6%. The theoretical prediction from Friar and Rosen [24] is shown in the right panel of Fig. 2 for 374.5 MeV and 747.2 MeV: **the expected (constant) 2% predicted discrepancy is clearly not reproducing the magnitude and energy dependence behavior seen in the data.**

In the left panel of Fig. 3, we also compare the only datum measured with positrons to electrons [5]. Due to time constraint, the poor statistics led to a large error bar: $\sigma_{e^+}/\sigma_{stat} = (-44 \pm 30)\%$. Using a phase-shift analysis under the assumption that the inelastic excitation is represented by a single monopole transition and that the nuclear excitation energy can be neglected, Rawitscher [26] predicts a small effect inside the first minimum of diffraction, around 5% (Fig. 3, right panel). Furthermore, the same sign and amplitude is expected for both electrons and positrons for 250 MeV electrons and positrons incident on ^{40}Ca inside the minimum while there should be opposite signs outside, in contradiction with the experimental observation.

> **The sign of the dispersive effects as a function of the lepton probe (e.g., $e^{\pm}$) is necessary to correctly understand their contributions within and outside minima of diffraction.**

2.2 Impacts on the nuclear matter

The dispersive cross section $\sigma_{disp} = \sigma_{stat+disp} = \sigma_{exp}$ can be expressed as a function of the cross section σ_{stat}:

$$\sigma_{disp} = \sigma_{stat}[1 + \delta_{disp}(E_e)] \tag{8}$$

with $\delta_{disp}(E_e)$ the higher order correction to the Born Approximation, σ_{disp} obtained from experimental measurements, and σ_{stat} the expected cross section from the Born Approximation. Equation (8) states that the observed experimental cross sections could be modeled by a small multiplicative perturbation added to the static cross section.

2.2.1 Effects on nuclear radii

In the Plane Wave Born Approximation, the nuclear charge density distribution $\rho_{\rm ch}(r)$ is the Fourier transform of the nuclear form factor and for spherically symmetric charge distributions the relation is [27]:

$$\rho_{\rm ch}(r) = \frac{1}{2\pi^2} \int F_{\rm ch}(q) \frac{\sin(qr)}{qr} q^2 dq \tag{9}$$

$\rho_{\rm ch}(r)$ can thus be extracted from the experimentally measured $F_{\rm ch}(q^2)$ and it is usually normalized to either 1 or the total charge of the nucleus. A model independent analysis can be done to extract the nuclear charge density distributions using either a sum of Gaussian (SOG) [28] or sum of Bessel (FB) [29] functions [27]. One can use the zero'th spherical Bessel function $j_0(r) = \sin(qr)/qr$ to expand the charge density as:

$$\rho_{\rm ch}^{\rm FB}(r) = \begin{cases} \sum_\nu a_\nu j_0\left(\frac{\nu\pi r}{R_{\rm cut}}\right) & \text{for} \quad r \le R_{\rm cut} \\ 0 & \text{for} \quad r > R_{\rm cut} \end{cases} \tag{10}$$

with $R_{\rm cut}$ the cut-off radius chosen such as the charge distribution is zero beyond that value and the coefficients a_ν related to the form factor as $a_\nu = q_\nu^2 F_{\rm ch}(q_\nu)/2\pi R_{cut}$, where $q_\nu = \nu\pi/R_{cut}$ is obtained from the ν-th zero of the Bessel function j_0.

Ignoring the contribution of the neutrons to the electric charge distribution of the nucleus, $\rho_{\rm ch}(r)$ could be considered as resulting from folding the distribution $\rho_{\rm nuc}(r)$ of the protons inside the nucleus with the finite extension of the protons $\rho_p(r)$ [29]. The Fourier transform of $\rho_{\rm ch}(r)$ is then given by the product of the transform of $\rho_{\rm nuc}(r)$ and $\rho_p(r)$:

$$F_{\rm ch}(q) = F_{\rm nuc}(q) F_p(q) \tag{11}$$

The relationship between the corresponding radii is:

$$R_{\rm ch}^2 = R_{\rm nuc}^2 + R_p^2 \tag{12}$$

with $R_p = 0.8414(19)$ fm the proton radius [30]. The rms $\langle r_{\rm ch}^2 \rangle^{1/2}$ is then:

$$\langle r^2_{\rm ch}\rangle = \int_0^{R_{\rm cut}} \rho_{\rm ch}(r) r^2 d^3r = 4\pi \int_0^{R_{\rm cut}} \rho_{\rm ch}(r) r^4 dr = \langle r^2_{\rm ch}\rangle = 4\pi \sum_\nu a_\nu \frac{(-1)^\nu R^5_{\rm cut}(6-\nu^2\pi^2)}{\nu^4\pi^4} \tag{13}$$

Therefore, all the coefficients a_ν of the Fourier Bessel expansion play a role in estimating the radius of the charge density distribution, decreasing in importance as $1/\nu^2$. If the measured cross sections used to extract the value of the form factor $F_{\rm ch}(q)$ are indeed modified by the dispersive corrections, then the change would propagate through the fitted coefficients a_ν to the estimate of the charge radius $R_{\rm ch} \equiv \langle r^2_{\rm ch}\rangle^{1/2}$. The total change in $R_{\rm ch}$ can be written as [31]:

$$\delta R_{ch} = \sum_i^N \frac{\partial R_{ch}}{\partial y_i}\delta y_i = \sum_i^N \Big(\sum_\nu^M \frac{\partial R_{ch}}{\partial a_\nu}\frac{\partial a_\nu}{\partial y_i}\Big)\delta y_i, \tag{14}$$

where δy_i is the change in the i$^{\rm th}$ value of the form factor $y_i = F(q_i)$, in this case due to the dispersive effects. If we assume that we can separate the total effect of the dispersive effects on the form factor values as:

$$F_{disp}(q) = F(q)_{stat}\left[1 + \frac{1}{2}\delta(E_e)S(q)\right], \tag{15}$$

with $\delta_{disp} = \delta(E_e)S(q)$ from Eq. (8) where $\delta(E_e)$ controls the overall strength of the perturbation and $S(q)$ controls the impact this change would have on different q values. The factor of 1/2 comes from assuming that $\delta(E_e)$ is small and propagating the change from Eqs. (1) and (8): $F \propto \sqrt{\sigma}$ which implies $\delta F/F \propto (1/2)\ \delta\sigma/\sigma$. One can then write the change in the charge radius as:

$$R^{disp}_{\rm ch} = R^{stat}_{\rm ch}\left[1 + \beta\delta(E_e)\right] \tag{16}$$

where β is a proportionality coefficient fixed once $S(q)$ is specified (e.g., for a given fixed strength $\delta(E_e)$, the change in the radius will depend on the shape of $S(q)$, which is encoded in β). The results

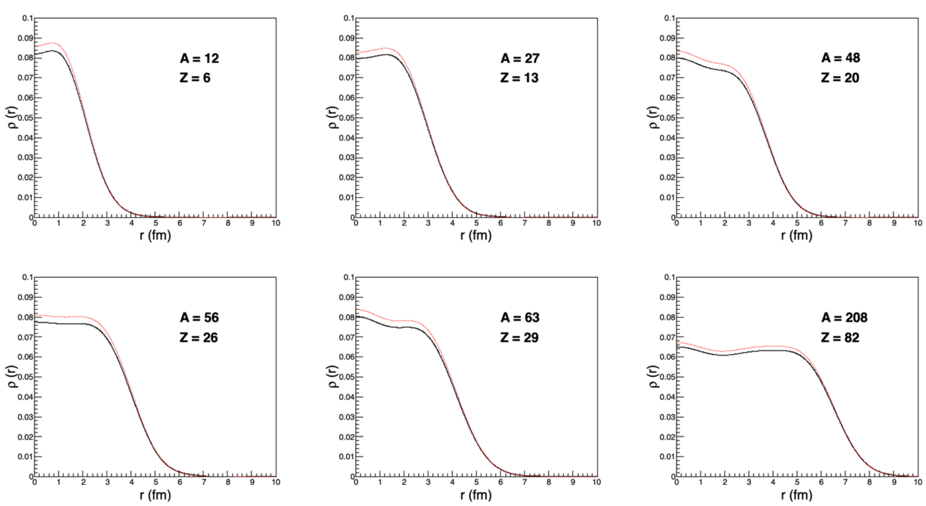

Figure 4: The modified charge distributions for ^{12}C, ^{27}Al, ^{48}Ca, ^{56}Fe, ^{63}Cu and ^{208}Pb. The changes were obtained using the empirical linear parameterization of the dispersive effects from [31].

from this study reported in Fig. 10 of [31] use three different test perturbations $S(q)$ plus an empirical one, when using the data without dispersive corrections from Offermann [4] for the central values of the form factor. For the three test cases these values were modified assuming a constant high value of $\delta(E_e) = 30\%$ (obtained from Fig. 2 above). When using the empirical perturbation for the δy_i in Eq. (14) an effect of 0.25% was found in the radius, very close to the actual 0.26% (reported as 0.28% when using rounded values for the radii) in [4].

Using the empirical linear parameterization of the dispersive effects from [31], $f_{emp}(q) = (1 - 0.00833q)$, the modification of the nuclear charge distribution is shown on various nuclei in Fig. 4.

A recent technical workshop of the International Atomic Energy Agency on the compilation and evaluation of nuclear charge radii [32] highlighted the fact that published electron scattering data have not been corrected for dispersive corrections, thus affecting the absolute values published in the literature.

There is a critical need to enable access to both electron and positron beams for a systematic program that could accurately measure charge radii from electron scattering corrected from the contribution from dispersive corrections.

2.2.2 Neutron skin puzzle and single spin asymmetries

The Coulomb field extracted from $\langle r^2\rangle^{1/2}$ should also be modified

$$\mid V_C \mid = \mid V_C^{stat} \mid = \frac{KZ}{\langle r^2\rangle^{1/2}}\,;K = 1/4\pi\varepsilon_0 \longrightarrow \mid V_C^{disp} \mid = \mid V_C^{stat} \mid /[1+\beta\delta(E_e)] \tag{17}$$

In order to estimate the dispersive corrections for ^{208}Pb, a two-step approach is needed using Coulomb fields from [6]: (1) a scaling of the dispersive corrections from carbon to lead found to be around 8% [31] is compatible with the $\sim 6\%$ effect observed by Breton et al. [3]; and (2) applying this scaling to the value from Offermann et al. [4] leading to $0.28\% R_{\text{scale}} = 0.07\%$. The latest reported experimental value of the charge radius of lead is [33] $R_{\text{ch}} = 5.5012(13)$ fm which would imply an upward shift to 5.5053(13) fm when taking the 0.07% scaling into account.

The situation is far more complex for parity-violating experiments [34, 35, 36] from which the measured asymmetry is used to extract a neutron skin. These experiments typically occurred near diffractive minima to maximize their sensitivity to the physics [37], where also dispersive corrections contribute the most. The connection to the dispersive effects arises from single-spin asymmetries (SSA) of elastic electron scattering off nuclei (see Ref. [38]). Beam-normal SSA conserves parity, but it is zero in the first Born approximation (or one-photon exchange) and may be used as a probe of the absorptive (imaginary) part of the scattering amplitude. Thus, past JLab experiments that measured beam-normal SSA on nuclear targets [39, 40] provided unambiguous evidence of effects beyond the Born approximation. To describe these data on SSA, Coulomb distortions of the electron's wave function appear to be insufficient, and excitation of nuclei during the scattering process played a defining role in the observed agreement between the experimental SSA data and theory. However, although good agreement with the theory was observed for light nuclei [39, 40], the situation with ^{208}Pb was not satisfactory even after consideration of combined effects of the electron wave distortion and nuclear excitations [41]. To address this apparent "^{208}Pb-puzzle", a new measurement of beam-normal SSA on a range on nuclei was approved by PAC52 at JLab [42].

The proposed experiment will probe both the real and imaginary parts of the scattering amplitude combined, providing for a complete description of the scattering process after comparing with experimental SSA data.

2.2.3 Coulomb Sum Rule (CSR)

It is defined as the integral of the longitudinal response function $R_L(\omega, |\mathbf{q}|)$ extracted from quasi-elastic electron scattering [43]:

$$S_L(|\mathbf{q}|) = \int_{\omega>0}^{|\mathbf{q}|} \frac{R_L(\omega, |\mathbf{q}|)}{ZG_{E_p}^2(Q^2) + NG_{E_n}^2(Q^2)} d\omega \tag{18}$$

where $-Q^2 = \omega^2 - \vec{q}^2$ with ω the energy transfer and $\vec{q}$ the three-momentum transfer. $G_{E_{p,n}}(Q^2)$ is the proton (neutron) form factor which reduces to the Sachs electric form factor if the nucleon is not modified by the nuclear medium [44]. $\omega > 0$ ensures that the integration is performed above the elastic peak. In essence, CSR states that by integrating the longitudinal strength over the full range of energy loss ω at large enough momentum transfer q, one should get the total charge (number of protons) of a nucleus.

The quenching of CSR has been found to be as much as 30% [45] for medium and heavy nuclei. Using a quantum field-theoretic quark-level approach which preserves the symmetries of quantum chromodynamics, as well as exhibiting dynamical chiral symmetry breaking and quark confinement, the most recent calculation by Cloet et al. [46] confirmed the dramatic quenching of the Coulomb Sum Rule for momentum transfers $|q| \gtrsim 2.5$ fm^{-1} that lies in changes to the proton Dirac form factor induced by the nuclear medium.

In quasi-elastic electron scattering, the nuclear response is affected by the fact that nucleons are not free and carry a momentum distribution, the existence of nucleon-nucleon interactions and interactions between the incoming and outgoing probe and recoils. Therefore, noting that R_L probes $\rho_{\mathrm{nuc}} = \rho_{\mathrm{protons}}$ while elastic scattering experiments probe $\rho_{\mathrm{ch}}(r)$, any measured shift of $F_{ch}(q)$ results from a change in F_{nuc} or F_p, or both. Even when considering the contribution from two-photon exchanges, the discrepancy observed cannot explain the 30% quenching of R_L [20, 21, 22].

Assuming that the contribution from dispersive effects found in $\rho_{\mathrm{ch}}(r)$ translates entirely in a change in ρ_{protons} and hence in the CSR, our naive model described above gives (with nuc = p or n):

$$G^{disp}_{E_{\mathrm{nuc}}}(Q^2) = \frac{G^{stat}_{E_{\mathrm{nuc}}}(Q^2)}{1+\beta\delta(E_e)} \tag{19}$$

Hence:

$$S^{disp}_L(|\mathbf{q}|) = S^{stat}_L(|\mathbf{q}|) \ \times \ [1+\beta\delta(E_e)] \tag{20}$$

Using Fig. 2 for a 600 MeV incident beam on ^{12}C (same kinematic regime as [47]), one would expect a 15% correction in the minimum of diffraction, which is a factor of 7.5 from the 2% prediction from Friar and Rosen [24]. Above the minimum, their prediction indicates an almost linear increase of the dispersion corrections up to about 3.3 fm^{-1} where it reaches a maximum of about 3%. Assuming the same scaling, that is a $0.03 \times 7.5 \simeq 22\%$ predicted effect for ^{12}C at this energy [47].

Dispersive effects could have a non-negligible contribution to the CSR. Mapping their contributions for various nuclei in quasi-elastic scattering could shed light on the long standing quenching of the nuclear longitudinal response.

2.2.4 Rare isotopes and the nuclear structure

The understanding of the inner structure of nuclei is primary done through break-up and pick-up reactions using heavy-ion collisions and fragmentation processes [48]. These experiments produce rare isotopes at facilities such as the Facility for Antiproton and Ion Research (FAIR) [49], the Institute of Physical and Chemical Research or Rikagaku Kenkyūsho (RIKEN) [50] and the Facility for Rare Isotope Beams (FRIB) [51]. The theoretical description of these reactions is often based on mean field nuclear interactions between the incoming ion and target nucleus. The understanding of peripheral heavy ion collisions involve both elastic and inelastic scattering processes. The treatment of the interaction requires knowledge of the relationship between the N-N interaction and the heavy ion optical potentials. When applicable, the approach uses a double-folding model in which the optical potential for the heavy ion scattering is obtained by averaging an appropriate N-N interaction over the matter distributions within the two colliding ions in the same way that the Coulomb interaction potential between two charge distributions is obtained by averaging the point-charge r^{-1} interaction over the distributions. See Refs. [52, 53] for more details. The optical potentials contains real (Coulomb, U_C) and imaginary (nuclear, U_I) parts: U_C takes into account the charge distributions of the projectile and target nuclei while U_I includes the treatment of the nucleon-nucleon interaction.

The charge density (for both projectile and target) enters implicitly in U_C and is usually taken from electron scattering data when available. An average global parameterization is often used from a two-Fermi parameter distribution [53]:

$$\rho(r) = \frac{\rho_0}{1+e^{\left(\frac{r-R_0}{a}\right)}} \tag{21}$$

with $R_0 = 1.76Z^{1/3} - 0.96$ fm and the average diffuseness value $a = 0.53$ fm.

In Fig. 5, we compare the elastic angular distribution of ^{33}Mg off a 1 mm thick ^{9}Be at 88.8 MeV/u using the MoNA-LISA-Sweeper setup at NSCL [55]. The reconstructed form factor was normalized to 1 and uses the COSY optical matrix of the large gap sweeper magnet (see the experimental setup in [55]) before (open blue circles) and after (filled red circles) adjusting the COSY matrix elements to optimize the event reconstruction. The data are compared to a preliminary prediction from Capel [56]

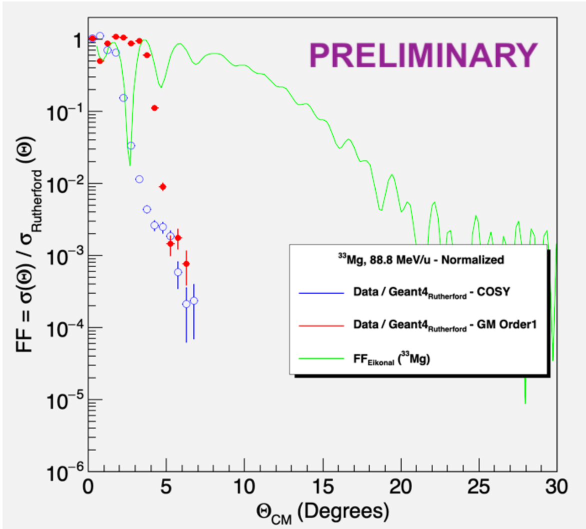

Figure 5: Preliminary angular distribution of ^{9}Be(^{33}Mg,^{33}Mg) at 88.8 MeV/u using the MoNA-LISA-Sweeper setup at NSCL [54]. See text for details.

using an eikonal approach. The distribution shows up to the third diffraction minimum which can be used to extract the matter radii of this nucleus.

The ability to reconstruct the elastic angular distribution of rare isotopes at FRIB is part of a new effort within the MoNA Collaboration [57]. Thanks to its segmented target [54, 58], there is some sensitivity to possibly obtain information about nuclear matter radii of such isotopes even within the small acceptance of the sweeper magnet ($\Theta_{lab} \lesssim 8°$). The neutron distributions are a critical ingredients for theoretical models in order to properly describe nucleus-nucleus interactions (coulomb and nuclear): obtaining the charge distribution (from electron/positron elastic scattering) and matter distribution (from elastic nucleus-nucleus scattering) would provide a pathway to gain some access to the neutron distributions within stable and unstable nuclei.

As previously noted in section 2.2.1, accurate determination of the nuclear charge distribution corrected for dispersive effects is vital for proper theoretical descriptions of the nuclear matter.

2.2.5 Electron dipole moment

The electromagnetic current, taking into account spin coupling, can be expressed as [59]

$$\begin{aligned}\bar{u}(\mathbf{p_1})\mathcal{O}^{\mu}(l,q)u(\mathbf{p_2}) &= \bar{u}(\mathbf{p_1})\left\{F_1(q^2)\gamma^{\mu} + \frac{i\sigma^{\mu\nu}}{2m}q_{\nu}F_2(q^2)\right.\\ &+ \left. i\varepsilon^{\mu\nu\alpha\beta}\frac{\sigma_{\alpha\beta}}{4m}q_{\nu}F_3(q^2) + \frac{1}{2m}\left(q^{\mu} - \frac{q^2}{2m}\gamma^{\mu}\right)\gamma_5 F_4(q^2)\right\}u(\mathbf{p_2})\end{aligned}$$

The four form factors are related to the charge (F_1), magnetic moment (F_2), electron dipole moment (F_3) and anapole moment (F_4). The first two have been extensively measured and the discrepancy observed when comparing the G_E/G_M ratio from unpolarized and polarized experiments is at the origin of the two-photon exchange relevancy in elastic electron scattering. The latter two are small: the G0 and SAMPLE experiments [60] provided insights into F_4. In order to probe these form factors, polarized electrons and positron beams are required.

The proposed experiment will not measure these form factors and evaluate the amplitude of dispersive corrections in spin-polarized observables as only unpolarized beams is being requested here. However, using data from our non-spin 0 targets will provide some sensitivity to the evolution of dispersive corrections to spin observables, especially regarding F_3.

3 Experimental Details

The proposed experiment will provide information about the magnitude and energy dependence of the dispersive effects through inclusive $A(e^{\pm}, e^{\pm})$ unpolarized elastic scattering around the first and second diffraction minima of eight nuclei (^{12}C, ^{27}Al, ^{63}Cu, ^{48}Ca, ^{56}Fe, ^{196}Pt, ^{208}Pb and ^{209}Bi) at four incident beam energies of 0.70, 1.06, 2.12 and 4.24 GeV. The non-spin 0 targets, aluminum (spin 5/2), copper (spin 3/2) and bismuth (spin 5/2) will be used to extract some sensitivity to spin-observables and an upper limit on EDM.

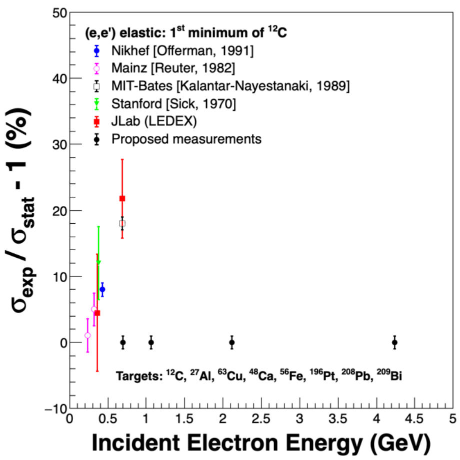

Figure 6: The projected $A(e, e')$ measurements for 0.70, 1.06, 2.12 and 4.24 GeV incident electron/positron beam energies.

3.1 Required Equipment

The experiment will be performed in two phases in the experimental Hall C using the Super High Momentum Spectrometer (SHMS) at Jefferson Lab in normal configuration with its standard detector systems:

Phase 1: electron beams at high current will measure $A(e^-, e^-)$ cross sections with currents of $0.1 - 100$ μA to provide relative information about dispersive effects by comparing measured cross sections to theoretical calculations.

Phase 2: electron and positron beams at low current will measure $A(e^{\pm}, e^{\pm})$ cross sections acquired with beam currents of $0.1 - 1$ μA to extract the absolute magnitude of dispersive effects.

3.2 Statistics and Systematics

The in-house SIMC Monte Carlo simulation was used to estimate the beam time needed to acquire 10^6 events (phase 1) and 10^4 events (phase 2) at each kinematic setting. The simulation includes the SHMS momentum and acceptance resolution, radiative corrections and utilizes the deForest elastic cross section formalism.

	Phase 1 (%)	**Phase 2 (%)**
Statistics	0.1	1.0
Acceptance	1.0	1.0
Tracking Efficiency	0.5	0.5
Radiative corr.	1.2	1.2
Target Thickness	0.5	0.5
Total	1.7	2.0

Table 1: The estimated dominating statistical and systematic errors.

The kinematics were calculated using a phase shift analysis code and Bessel parameterizations of the charge distributions from deVries [27]. The thickness for each target was taken to be 225 mg/cm^2, similar to prior measurements performed in the first minimum of ^{12}C [5, 6]. The error budget on the measured cross sections is listed in Table 1: the estimated errors are around 1.7% for A(e^-, e^-) and 2.0% for A$(e^\pm, e^\pm)$, respectively.

3.3 Kinematics

The corresponding kinematics are listed in Table 2 (phase 1) and Table 3 (phase 2). The four-momentum transfer (q) and location of the 1$^{\text{st}}$(q^1_{min}) and 2$^{\text{nd}}$(q^2_{min}) minima of diffraction are also provided. The rates for phase 1 range from 8.4×10^{10} Hz at small angles to 2.8 Hz at large angles. To accommodate these high rates, the beam current will be adjusted from 100 μA to 10 μA and sometimes 100 nA for some kinematics. For phase 2, the maximum current is expected to be around 1 μA: we will restrict our statistics to 10^4 events for both beams, thus increasing our statistical error from 0.1% to 1.0%, as well as lowered the current for some of the small angles to 100 nA as the rates are still above the 1 MHz detectors limit.

Phase 1: A(e^-, e^-) for 100 μA					
Target	**E$_e$ (GeV)**	**$\theta_{e'}$ (Deg.)**	**q-range (fm^{-1})**	**q^1_{min}/q^2_{min} (fm^{-1})**	**Rates (Hz)**
^{12}C	0.700	20,25,30,35,40	1.2-2.4	1.8	$2.8 - 1.3 \times 10^6$
^{27}Al		15,20,22.5,25,30	0.9-1.8	1.2	$2.6 \times 10^3 - 3.6 \times 10^7$
^{48}Ca		5.5,7.5,10,12.5,15	0.3-0.9	0.4/0.8	$2.6 \times 10^7 - 3.6 \times 10^{10}$
^{56}Fe		5.5,10,15,25	0.3-1.5	1.1	$6.8 \times 10^4 - 5.6 \times 10^{10}$
^{63}Cu		5.5,10,15,20,25	0.6-1.5	0.95	$4.8 \times 10^4 - 1.2 \times 10^9$
^{196}Pt		5.5,10,15,20	0.3-1.5	0.4/0.9	$8.4 \times 10^5 - 8.2 \times 10^{10}$
^{208}Pb		5.5,10,15,20	0.3-1.2	0.4/0.8	$8.1 \times 10^5 - 8.3 \times 10^{10}$
^{209}Bi		5.5,7.5,10,12.5	0.3-0.8	0.3/0.5	$1.6 \times 10^8 - 8.4 \times 10^{10}$
^{12}C	1.060	10,15,20,25,30	0.9-2.8	1.8	$20.8 - 5.2 \times 10^7$
^{13}Al		5.5,10,15,20	0.5-1.9	1.2	$19.9 - 7.0 \times 10^9$
^{48}Ca		5.5,10	0.5-0.9	0.4/0.8	$4.2 \times 10^6 - 6.6 \times 10^9$
^{56}Fe		5.5,10,15	0.5-1.4	1.1	$6.1 \times 10^5 - 1.0 \times 10^{10}$
^{63}Cu		5.5,10,15,20,25	0.5-2.3	0.95	$12.3 - 9.3 \times 10^9$
^{196}Pt		5.5,10,15	0.5-1.4	0.4/0.9	$3.5 \times 10^6 - 1.0 \times 10^{10}$
^{208}Pb		5.5,10,15	0.5-1.4	0.4/0.8	$3.4 \times 10^6 - 1.0 \times 10^{10}$
^{209}Bi		5.5,10	0.5-0.9	0.3/0.5	$4.7 \times 10^7 - 1.0 \times 10^{10}$
^{12}C	2.120	5.5,7.5,10	1.0-1.9	1.8	$1.4 \times 10^4 - 7.8 \times 10^7$
^{12}C	4.240	5.5	2.1	1.8	6.5×10^3

Table 2: The proposed phase 1 elastic kinematics in A(e^-, e^-) for each target.

4 Beamtime Request

The requested beam time for the proposed measurements amounts to 18.24 days for A(e^-, e^-) in phase 1 and 29.24 days for A$(e^\pm, e^\pm)$ in phase 2, respectively. The details are listed in Table 4. We assumed 30 mins for magnetic field changes, 15 mins for spectrometer changes and 5 mins for target changes. For phase 2, we also assumed 2 hrs to switch between the lepton probes ($e^\pm$ to $e^\mp$) and the numbers provided are doubled to account for measurements during each beam. Furthermore, the beam current adjustments noted above for some kinematics due to the rate limitation required for the tracking detectors, $0.1 - 100$ μA (Table 2) and $0.1 - 1.0$ μA (Table 3), have been taken into account in our estimates. Prescales will also be used to keep the data acquisition rate within a reasonable

Phase 2: A($e^{\pm}, e^{\pm}$) for 1 μA				
Target	**E_e (GeV)**	**$\theta_{e'}$ (Deg.)**	**q-range (fm^{-1})**	**q^1_{min}/q^2_{min} (fm^{-1})**
^{12}C	0.700	20,25,30,35	1.2-2.1	1.8
^{27}Al		20,25,30	1.2-1.8	1.2
^{56}Fe		15,20	0.9-1.2	1.1
^{63}Cu		20,25,30	1.2-1.8	0.95/1.8
^{12}C	1.060	15,20,25	1.4-2.3	1.8
^{13}Al		15,20,25	1.4-2.3	1.2
^{56}Fe		15	1.4	1.1
^{63}Cu		15,17.5,20	1.4-1.9	0.95/1.8
^{196}Pt		10,12.5,15	0.9-1.4	0.4/0.9
^{208}Pb		12.5	1.2	0.4/0.8
^{12}C	2.120	7.5,10,12.5	1.4-2.3	1.8
^{12}C	4.240	5.5	2.1	1.8

Table 3: The proposed phase 2 elastic kinematics in A($e^{\pm}, e^{\pm}$) for each target.

range. This experiment is also self-calibrating through the data on the ^{12}C target. Finally, we are investigating using the HMS spectrometer running in parallel to optimize/minimize the requested times. For example, the HMS could not only be used for large angle measurements but also serve as a cross-calibrating device at specific momentum transfers. These were not taken into account for the current estimates.

Energy (GeV)	**Description**	**A(e^-, e^-) (days)**	**A($e^{\pm}, e^{\pm}$) (days)**
0.70	Production	6.19	1.60
	Spectrometer Rotation	0.38	0.13
	Spectrometer Settings	0.75	0.25
	Target Change	0.03	0.01
	Beam switch ($e^{\pm} \leftrightarrow e^{\mp}$)	-	0.16
1.06	Production	8.21	24.0
	Spectrometer Rotation	0.30	0.15
	Spectrometer Settings	0.60	0.29
	Target Change	0.03	0.02
	Beam switch ($e^{\pm} \leftrightarrow e^{\mp}$)	-	0.16
2.12	Production	0.60	2.04
	Spectrometer Rotation	0.03	0.03
	Spectrometer Settings	0.06	0.06
	Target Change	0.003	0.003
	Beam switch ($e^{\pm} \leftrightarrow e^{\mp}$)	-	0.16
4.24	Production	1.02	0.02
	Spectrometer Rotation	0.01	0.01
	Spectrometer Settings	0.02	0.02
	Target Change	0.003	0.003
	Beam switch ($e^{\pm} \leftrightarrow e^{\mp}$)	-	0.16
Total		**18.24 days**	**29.24 days**

Table 4: Beam time request.

5 Summary

We propose to map out the magnitude of dispersive effects, e.g., measure both their real and imaginary parts that enter into the scattering amplitude, through unpolarized inclusive $A(e,e')$ electron and positron elastic scattering around the first and second diffraction minima of eight nuclei (^{12}C, ^{27}Al, ^{63}Cu, ^{48}Ca, ^{56}Fe, ^{196}Pt, ^{208}Pb and ^{209}Bi) for four incident beam energies (0.70, 1.06, 2.12, and 4.24 GeV) in the experimental Hall C at Jefferson Lab. This will be accomplished in two phases: the first phase will provide qualitative information about these effects from $A(e^-,e^-)$ by comparing the measured cross sections to theoretical calculations while the second phase will measure the absolute magnitude of these effects by comparing the cross sections from $A(e^-,e^-)$ and $A(e^+,e^+)$. **We request 18 days (phase 1) and 29 days (phase 2) to perform these measurements that will consist of the first ever comprehensive study and energy dependence of dispersive effects.**

References

[1] L. S. Cardman, J. W. Lightbody, S. Penner, S. P. Fivozinsky, X. K. Maruyama, W. P. Trower, and S. E. Williamson. The charge distribution of 12 C. *Phys. Lett.*, 91B:203–206, 1980.

[2] E.A.J.M. Offermann, L.S. Cardman, H.J. Emrich, G. Fricke, C.W. deJager, H. Miska, D. Rychel, and H. deVries. Search for Dispersive Effects in Elastic Electron Scattering From ^{12}C. *Phys. Rev. Lett.*, 57:1546–1549, 1986.

[3] V. Breton, P. Bricault, L. S. Cardman, B. Frois, D. Goutte, D. B. Isabelle, A. J. Linzey, G. Masson, L. C. Maximon, E. A. J. M. Offermann, X. H. Phan, S. K. Platchkov, I. Sick, and S. E. Williamson. High-accuracy comparison of electron and positron scattering from nuclei. *Phys. Rev. Lett.*, 66:572–575, Feb 1991.

[4] E. A. J. M. Offermann, L. S. Cardman, C. W. de Jager, H. Miska, C. de Vries, and H. de Vries. Energy dependence of the form-factor for elastic electron scattering from C-12. *Phys. Rev.*, C44:1096–1117, 1991.

[5] P. Guèye, M. Bernheim, J. F. Danel, J. E. Ducret, L. Lakéhal-Ayat, J. M. Le Goff, A. Magnon, C. Marchand, J. Morgenstern, J. Marroncle, P. Vernin, A. Zghiche-Lakéhal-Ayat, V. Breton, S. Frullani, F. Garibaldi, F. Ghio, M. Jodice, D. B. Isabelle, Z. E. Meziani, E. Offermann, and M. Traini. Dispersive effects from a comparison of electron and positron scattering from ^{12}C. *Phys. Rev. C*, 57:2107–2110, May 1998.

[6] P. Guèye, M. Bernheim, J. F. Danel, J. E. Ducret, L. Lakéhal-Ayat, J. M. Le Goff, A. Magnon, C. Marchand, J. Morgenstern, J. Marroncle, P. Vernin, A. Zghiche-Lakéhal-Ayat, V. Breton, S. Frullani, F. Garibaldi, F. Ghio, M. Iodice, D. B. Isabelle, Z.-E. Meziani, E. Offermann, and M. Traini. Coulomb distortion measurements by comparing electron and positron quasielastic scattering off ^{12}C and ^{208}Pb. *Phys. Rev. C*, 60:044308, Sep 1999.

[7] I. Sick and J. S. Mccarthy. Elastic electron scattering from c-12 and o-16. *Nucl. Phys.*, A150:631–654, 1970.

[8] Pierre A. M. Guichon and M. Vanderhaeghen. How to reconcile the Rosenbluth and the polarization transfer method in the measurement of the proton form-factors. *Phys. Rev. Lett.*, 91:142303, 2003.

[9] P. G. Blunden, W. Melnitchouk, and J. A. Tjon. Two photon exchange and elastic electron proton scattering. *Phys. Rev. Lett.*, 91:142304, 2003.

[10] Michail P. Rekalo and Egle Tomasi-Gustafsson. Polarization observables in the processes p + p $\rightarrow$ Theta+ + Sigma+ and n + p $\rightarrow$ Theta+ + Lambda0, for any spin and parity of the Theta+ hyperon in the threshold region. *Eur. Phys. J.*, A22:119–124, 2004.

[11] Y. C. Chen, A. Afanasev, S. J. Brodsky, C. E. Carlson, and M. Vanderhaeghen. Partonic calculation of the two photon exchange contribution to elastic electron proton scattering at large momentum transfer. *Phys. Rev. Lett.*, 93:122301, 2004.

[12] Andrei V. Afanasev and N. P. Merenkov. Large logarithms in the beam normal spin asymmetry of elastic electron-proton scattering. *Phys. Rev.*, D70:073002, 2004.

[13] J. Arrington. Extraction of two-photon contributions to the proton form-factors. *Phys. Rev.*, C71:015202, 2005.

[14] P. G. Blunden, W. Melnitchouk, and J. A. Tjon. Two-photon exchange in elastic electron-nucleon scattering. *Phys. Rev.*, C72:034612, 2005.

[15] P. G. Blunden and W. Melnitchouk. Dispersive approach to two-photon exchange in elastic electron-proton scattering. *Phys. Rev.*, C95(6):065209, 2017.

[16] D. Adikaram, D. Rimal, L. B. Weinstein, B. Raue, P. Khetarpal, R. P. Bennett, J. Arrington, W. K. Brooks, K. P. Adhikari, A. V. Afanasev, M. J. Amaryan, M. D. Anderson, S. Anefalos Pereira, H. Avakian, J. Ball, M. Battaglieri, I. Bedlinskiy, A. S. Biselli, J. Bono, S. Boiarinov, W. J. Briscoe, V. D. Burkert, D. S. Carman, S. Careccia, A. Celentano, S. Chandavar, G. Charles, L. Colaneri, P. L. Cole, M. Contalbrigo, V. Crede, A. D'Angelo, N. Dashyan, R. De Vita, E. De Sanctis, A. Deur, C. Djalali, G. E. Dodge, R. Dupre, H. Egiyan, A. El Alaoui, L. El Fassi, L. Elouadrhiri, P. Eugenio, G. Fedotov, S. Fegan, A. Filippi, J. A. Fleming, A. Fradi, B. Garillon, G. P. Gilfoyle, K. L. Giovanetti, F. X. Girod, J. T. Goetz, W. Gohn, E. Golovatch, R. W. Gothe, K. A. Griffioen, B. Guegan, M. Guidal, L. Guo, K. Hafidi, H. Hakobyan, C. Hanretty, N. Harrison, M. Hattawy, K. Hicks, M. Holtrop, S. M. Hughes, C. E. Hyde, Y. Ilieva, D. G. Ireland, B. S. Ishkhanov, D. Jenkins, H. Jiang, H. S. Jo, K. Joo, S. Joosten, N. Kalantarians, D. Keller, M. Khandaker, A. Kim, W. Kim, A. Klein, F. J. Klein, S. Koirala, V. Kubarovsky, S. E. Kuhn, K. Livingston, H. Y. Lu, I. J. D. MacGregor, N. Markov, P. Mattione, M. Mayer, B. McKinnon, M. D. Mestayer, C. A. Meyer, M. Mirazita, V. Mokeev, R. A. Montgomery, C. I. Moody, H. Moutarde, A. Movsisyan, C. Munoz Camacho, P. Nadel-Turonski, S. Niccolai, G. Niculescu, M. Osipenko, A. I. Ostrovidov, K. Park, E. Pasyuk, C. Peña, S. Pisano, O. Pogorelko, J. W. Price, S. Procureur, Y. Prok, D. Protopopescu, A. J. R. Puckett, M. Ripani, A. Rizzo, G. Rosner, P. Rossi, P. Roy, F. Sabatié, C. Salgado, D. Schott, R. A. Schumacher, E. Seder, Y. G. Sharabian, A. Simonyan, I. Skorodumina, E. S. Smith, G. D. Smith, D. I. Sober, D. Sokhan, N. Sparveris, S. Stepanyan, P. Stoler, S. Strauch, V. Sytnik, M. Taiuti, Ye Tian, A. Trivedi, M. Ungaro, H. Voskanyan, E. Voutier, N. K. Walford, D. P. Watts, X. Wei, M. H. Wood, N. Zachariou, L. Zana, J. Zhang, Z. W. Zhao, and I. Zonta. Towards a resolution of the proton form factor problem: New electron and positron scattering data. *Phys. Rev. Lett.*, 114:062003, Feb 2015.

[17] I. A. Rachek, J. Arrington, V. F. Dmitriev, V. V. Gauzshtein, R. E. Gerasimov, A. V. Gramolin, R. J. Holt, V. V. Kaminskiy, B. A. Lazarenko, S. I. Mishnev, N. Yu. Muchnoi, V. V. Neufeld, D. M. Nikolenko, R. Sh. Sadykov, Yu. V. Shestakov, V. N. Stibunov, D. K. Toporkov, H. de Vries, S. A. Zevakov, and V. N. Zhilich. Measurement of the two-photon exchange contribution to the elastic $e^{\pm}p$ scattering cross sections at the vepp-3 storage ring. *Phys. Rev. Lett.*, 114:062005, Feb 2015.

[18] B. S. Henderson, L. D. Ice, D. Khaneft, C. O'Connor, R. Russell, A. Schmidt, J. C. Bernauer, M. Kohl, N. Akopov, R. Alarcon, O. Ates, A. Avetisyan, R. Beck, S. Belostotski, J. Bessuille, F. Brinker, J. R. Calarco, V. Carassiti, E. Cisbani, G. Ciullo, M. Contalbrigo, R. De Leo, J. Diefenbach, T. W. Donnelly, K. Dow, G. Elbakian, P. D. Eversheim, S. Frullani, Ch. Funke, G. Gavrilov, B. Gläser, N. Görrissen, D. K. Hasell, J. Hauschildt, Ph. Hoffmeister, Y. Holler, E. Ihloff, A. Izotov, R. Kaiser, G. Karyan, J. Kelsey, A. Kiselev, P. Klassen, A. Krivshich, I. Lehmann, P. Lenisa, D. Lenz, S. Lumsden, Y. Ma, F. Maas, H. Marukyan, O. Miklukho, R. G. Milner, A. Movsisyan, M. Murray, Y. Naryshkin, R. Perez Benito, R. Perrino, R. P. Redwine, D. Rodríguez Piñeiro, G. Rosner, U. Schneekloth, B. Seitz, M. Statera, A. Thiel, H. Vardanyan, D. Veretennikov, C. Vidal, A. Winnebeck, and V. Yeganov. Hard two-photon contribution to elastic lepton-proton scattering determined by the olympus experiment. *Phys. Rev. Lett.*, 118:092501, Mar 2017.

[19] D. Rimal, D. Adikaram, B. A. Raue, L. B. Weinstein, J. Arrington, W. K. Brooks, M. Ungaro, K. P. Adhikari, A. V. Afanasev, Z. Akbar, S. Anefalos Pereira, R. A. Badui, J. Ball, N. A. Baltzell, M. Battaglieri, V. Batourine, I. Bedlinskiy, A. S. Biselli, S. Boiarinov, W. J. Briscoe, S. Bültmann, V. D. Burkert, D. S. Carman, A. Celentano, T. Chetry, G. Ciullo, L. Clark, L. Colaneri, P. L. Cole,

N. Compton, M. Contalbrigo, O. Cortes, V. Crede, A. D'Angelo, N. Dashyan, R. De Vita, A. Deur, C. Djalali, R. Dupre, H. Egiyan, A. El Alaoui, L. El Fassi, P. Eugenio, E. Fanchini, G. Fedotov, R. Fersch, A. Filippi, J. A. Fleming, T. A. Forest, A. Fradi, N. Gevorgyan, Y. Ghandilyan, G. P. Gilfoyle, K. L. Giovanetti, F. X. Girod, C. Gleason, W. Gohn, E. Golovatch, R. W. Gothe, K. A. Griffioen, L. Guo, K. Hafidi, C. Hanretty, N. Harrison, M. Hattawy, D. Heddle, K. Hicks, M. Holtrop, S. M. Hughes, Y. Ilieva, D. G. Ireland, B. S. Ishkhanov, E. L. Isupov, D. Jenkins, H. Jiang, S. Joosten, D. Keller, G. Khachatryan, M. Khandaker, W. Kim, A. Klein, F. J. Klein, V. Kubarovsky, S. E. Kuhn, S. V. Kuleshov, L. Lanza, P. Lenisa, K. Livingston, H. Y. Lu, I. J. D. MacGregor, N. Markov, B. McKinnon, M. D. Mestayer, M. Mirazita, V. Mokeev, A. Movsisyan, E. Munevar, C. Munoz Camacho, P. Nadel-Turonski, A. Ni, S. Niccolai, G. Niculescu, I. Niculescu, M. Osipenko, A. I. Ostrovidov, M. Paolone, R. Paremuzyan, K. Park, E. Pasyuk, W. Phelps, S. Pisano, O. Pogorelko, J. W. Price, Y. Prok, D. Protopopescu, A. J. R. Puckett, A. Rizzo, G. Rosner, P. Rossi, P. Roy, F. Sabatié, C. Salgado, R. A. Schumacher, E. Seder, Y. G. Sharabian, Iu. Skorodumina, G. D. Smith, D. Sokhan, N. Sparveris, Ivana Stankovic, S. Stepanyan, S. Strauch, V. Sytnik, M. Taiuti, B. Torayev, H. Voskanyan, E. Voutier, N. K. Walford, D. P. Watts, X. Wei, M. H. Wood, N. Zachariou, L. Zana, J. Zhang, Z. W. Zhao, and I. Zonta. Measurement of two-photon exchange effect by comparing elastic $e^{\pm}p$ cross sections. *Phys. Rev. C*, 95:065201, Jun 2017.

[20] Carl E. Carlson and Marc Vanderhaeghen. Two-Photon Physics in Hadronic Processes. *Ann. Rev. Nucl. Part. Sci.*, 57:171–204, 2007.

[21] J. Arrington, P. G. Blunden, and W. Melnitchouk. Review of two-photon exchange in electron scattering. *Prog. Part. Nucl. Phys.*, 66:782–833, 2011.

[22] A. Afanasev, P. G. Blunden, D. Hasell, and B. A. Raue. Two-photon exchange in elastic electron–proton scattering. *Prog. Part. Nucl. Phys.*, 95:245–278, 2017.

[23] Andreas Aste, Cyrill von Arx, and Dirk Trautmann. Coulomb distortion of relativistic electrons in the nuclear electrostatic field. *Eur. Phys. J.*, A26:167–178, 2005.

[24] James Lewis Friar and M. Rosen. Dispersion corrections to elastic electron scattering by C-12 and O-16. 2. on the use of the closure approximation. *Annals Phys.*, 87:289–326, 1974.

[25] Marco Traini. Coulomb distortion in quasielastic (e, e-prime) scattering on nuclei: Effective momentum approximation and beyond. *Nucl. Phys.*, A694:325–336, 2001.

[26] G. H. Rawitscher. Monopole excitation corrections to electron elastic scattering. *Phys. Rev.*, 151:846–852, Nov 1966.

[27] H. de Vries, C. W. de Jager, and C. de Vries. Nuclear Charge-Density-Distribution Parameters from Electron Scattering. *Atomic Data and Nuclear Data Tables*, 36:495, 1987.

[28] I. Sick. Model-independent nuclear charge densities from elastic electron scattering. *Nuclear Physics A*, 218(3):509 – 541, 1974.

[29] B. Dreher, J. Friedrich, K. Merle, H. Rothhaas, and G. Lührs. The determination of the nuclear ground state and transition charge density from measured electron scattering data. *Nuclear Physics A*, 235(1):219 – 248, 1974.

[30] CODATA18. Committee on data international science council, 2018 codata recommended values, 2018.

[31] P. Gueye, A. Kabir, P. Giuliani, J. Glister, B. Lee, R. Gilman, D. Higinbotham, E. Piasetzky, G. Ron, A. Sarty, W. Armstrong, J. Arrington, Z.-E. Meziani, and P. Solvignon. Dispersive corrections in elastic electron-nucleus scattering: An investigation in the intermediate energy regime and their impact on the nuclear matter. *European Physical Journal A: Hadrons and Nuclei*, 56(5):– , 126, May 2020. 10.1140/epja/s10050-020-00135-7.

[32] Jane Smith. Technical meeting on compilation and evaluation of nuclear charge radii, 2025.

[33] I. Angeli and K.P. Marinova. Table of experimental nuclear ground state charge radii: An update. *Atomic Data and Nuclear Data Tables*, 99(1):69 − 95, 2013.

[34] C. J. Horowitz et al. Weak charge form factor and radius of 208Pb through parity violation in electron scattering. *Phys. Rev.*, C85:032501, 2012.

[35] S. Abrahamyan, Z. Ahmed, H. Albataineh, K. Aniol, D. S. Armstrong, W. Armstrong, T. Averett, B. Babineau, A. Barbieri, V. Bellini, R. Beminiwattha, J. Benesch, F. Benmokhtar, T. Bielarski, W. Boeglin, A. Camsonne, M. Canan, P. Carter, G. D. Cates, C. Chen, J.-P. Chen, O. Hen, F. Cusanno, M. M. Dalton, R. De Leo, K. de Jager, W. Deconinck, P. Decowski, X. Deng, A. Deur, D. Dutta, A. Etile, D. Flay, G. B. Franklin, M. Friend, S. Frullani, E. Fuchey, F. Garibaldi, E. Gasser, R. Gilman, A. Giusa, A. Glamazdin, J. Gomez, J. Grames, C. Gu, O. Hansen, J. Hansknecht, D. W. Higinbotham, R. S. Holmes, T. Holmstrom, C. J. Horowitz, J. Hoskins, J. Huang, C. E. Hyde, F. Itard, C.-M. Jen, E. Jensen, G. Jin, S. Johnston, A. Kelleher, K. Kliakhandler, P. M. King, S. Kowalski, K. S. Kumar, J. Leacock, J. Leckey, J. H. Lee, J. J. LeRose, R. Lindgren, N. Liyanage, N. Lubinsky, J. Mammei, F. Mammoliti, D. J. Margaziotis, P. Markowitz, A. McCreary, D. McNulty, L. Mercado, Z.-E. Meziani, R. W. Michaels, M. Mihovilovic, N. Muangma, C. Muñoz Camacho, S. Nanda, V. Nelyubin, N. Nuruzzaman, Y. Oh, A. Palmer, D. Parno, K. D. Paschke, S. K. Phillips, B. Poelker, R. Pomatsalyuk, M. Posik, A. J. R. Puckett, B. Quinn, A. Rakhman, P. E. Reimer, S. Riordan, P. Rogan, G. Ron, G. Russo, K. Saenboonruang, A. Saha, B. Sawatzky, A. Shahinyan, R. Silwal, S. Sirca, K. Slifer, P. Solvignon, P. A. Souder, M. L. Sperduto, R. Subedi, R. Suleiman, V. Sulkosky, C. M. Sutera, W. A. Tobias, W. Troth, G. M. Urciuoli, B. Waidyawansa, D. Wang, J. Wexler, R. Wilson, B. Wojtsekhowski, X. Yan, H. Yao, Y. Ye, Z. Ye, V. Yim, L. Zana, X. Zhan, J. Zhang, Y. Zhang, X. Zheng, and P. Zhu. Measurement of the neutron radius of ^{208}Pb through parity violation in electron scattering. *Phys. Rev. Lett.*, 108:112502, Mar 2012.

[36] S. Abrahamyan, A. Acha, A. Afanasev, Z. Ahmed, H. Albataineh, K. Aniol, D. S. Armstrong, W. Armstrong, J. Arrington, T. Averett, B. Babineau, S. L. Bailey, J. Barber, A. Barbieri, A. Beck, V. Bellini, R. Beminiwattha, H. Benaoum, J. Benesch, F. Benmokhtar, P. Bertin, T. Bielarski, W. Boeglin, P. Bosted, F. Butaru, E. Burtin, J. Cahoon, A. Camsonne, M. Canan, P. Carter, C. C. Chang, G. D. Cates, Y.-C. Chao, C. Chen, J.-P. Chen, Seonho Choi, E. Chudakov, E. Cisbani, B. Craver, F. Cusanno, M. M. Dalton, R. De Leo, K. de Jager, W. Deconinck, P. Decowski, D. Deepa, X. Deng, A. Deur, D. Dutta, A. Etile, C. Ferdi, R. J. Feuerbach, J. M. Finn, D. Flay, G. B. Franklin, M. Friend, S. Frullani, E. Fuchey, S. A. Fuchs, K. Fuoti, F. Garibaldi, E. Gasser, R. Gilman, A. Giusa, A. Glamazdin, L. E. Glesener, J. Gomez, M. Gorchtein, J. Grames, K. Grimm, C. Gu, O. Hansen, J. Hansknecht, O. Hen, D. W. Higinbotham, R. S. Holmes, T. Holmstrom, C. J. Horowitz, J. Hoskins, J. Huang, T. B. Humensky, C. E. Hyde, H. Ibrahim, F. Itard, C.-M. Jen, E. Jensen, X. Jiang, G. Jin, S. Johnston, J. Katich, L. J. Kaufman, A. Kelleher, K. Kliakhandler, P. M. King, A. Kolarkar, S. Kowalski, E. Kuchina, K. S. Kumar, L. Lagamba, D. Lambert, P. LaViolette, J. Leacock, J. Leckey, J. H. Lee, J. J. LeRose, D. Lhuillier, R. Lindgren, N. Liyanage, N. Lubinsky, J. Mammei, F. Mammoliti, D. J. Margaziotis, P. Markowitz, M. Mazouz, K. McCormick, A. McCreary, D. McNulty, D. G. Meekins, L. Mercado, Z.-E. Meziani, R. W. Michaels, M. Mihovilovic, B. Moffit, P. Monaghan, N. Muangma, C. Muñoz Camacho, S. Nanda, V. Nelyubin, D. Neyret, Nuruzzaman, Y. Oh, K. Otis, A. Palmer, D. Parno, K. D. Paschke, S. K. Phillips, M. Poelker, R. Pomatsalyuk, M. Posik, M. Potokar, K. Prok, A. J. R. Puckett, X. Qian, Y. Qiang, B. Quinn, A. Rakhman, P. E. Reimer, B. Reitz, S. Riordan, J. Roche, P. Rogan, G. Ron, G. Russo, K. Saenboonruang, A. Saha, B. Sawatzky, A. Shahinyan, R. Silwal, J. Singh, S. Sirca, K. Slifer, R. Snyder, P. Solvignon, P. A. Souder, M. L. Sperduto, R. Subedi, M. L. Stutzman, R. Suleiman, V. Sulkosky, C. M. Sutera, W. A. Tobias, W. Troth, G. M. Urciuoli, P. Ulmer, A. Vacheret, E. Voutier, B. Waidyawansa, D. Wang, K. Wang, J. Wexler, A. Whitbeck, R. Wilson, B. Wojtsekhowski, X. Yan, H. Yao, Y. Ye, Z. Ye, V. Yim, L. Zana, X. Zhan, J. Zhang, Y. Zhang, X. Zheng, V. Ziskin, and P. Zhu. New measurements of the transverse beam asymmetry for elastic electron scattering from selected nuclei. *Phys. Rev. Lett.*, 109:192501, Nov 2012.

[37] J. Piekarewicz, A. R. Linero, P. Giuliani, and E. Chicken. Power of two: Assessing the impact of a second measurement of the weak-charge form factor of ^{208}Pb. *Phys. Rev. C*, 94:034316, Sep 2016.

[38] Andrei Afanasev, Jan C Bernauer, Peter Blunden, Johannes Blümlein, Ethan W Cline, Jan M Friedrich, Franziska Hagelstein, Tomáš Husek, Michael Kohl, Fred Myhrer, et al. Radiative corrections: from medium to high energy experiments. *Eur. Phys. J. A*, 60(4):91, 2024.

[39] S Abrahamyan, A Acha, A Afanasev, Z Ahmed, H Albataineh, K Aniol, DS Armstrong, W Armstrong, J Arrington, T Averett, et al. New measurements of the transverse beam asymmetry for elastic electron scattering from selected nuclei. *Phys. Rev. Lett.*, 109(19):192501, 2012.

[40] D Adhikari, H Albataineh, D Androic, K Aniol, DS Armstrong, Todd Averett, C Ayerbe Gayoso, S Barcus, V Bellini, RS Beminiwattha, et al. New measurements of the beam-normal single spin asymmetry in elastic electron scattering over a range of spin-0 nuclei. *Phys. Rev. Lett.*, 128(14):142501, 2022.

[41] Oleksandr Koshchii, Mikhail Gorchtein, Xavier Roca-Maza, and Hubert Spiesberger. Beam-normal single-spin asymmetry in elastic scattering of electrons from a spin-0 nucleus. *Phys. Rev. C*, 103(6):064316, 2021.

[42] (Spokepersons), C. Gal, C. Ghosh, and S. Park. Nuclear Dependence of Beam Normal Single Spin Asymmetry in Elastic Scattering from Nuclei. *Jefferson Lab Experiment E12-24-007*, August 2024.

[43] K. W. McVoy and L. Van Hove. Inelastic Electron-Nucleus Scattering and Nucleon-Nucleon Correlations. *Phys. Rev.*, 125:1034–1043, 1962.

[44] J. V. Noble. Modification of the nucleon's properties in nuclear matter. *Phys. Rev. Lett.*, 46:412–415, 1981.

[45] J. Morgenstern and Z. E. Meziani. Is the Coulomb sum rule violated in nuclei? *Phys. Lett.*, B515:269–275, 2001.

[46] Ian C. Cloët, Wolfgang Bentz, and Anthony W. Thomas. Relativistic and Nuclear Medium Effects on the Coulomb Sum Rule. *Phys. Rev. Lett.*, 116(3):032701, 2016.

[47] P. Barreau, M. Bernheim, J. Duclos, J.M. Finn, Z. Meziani, J. Morgenstern, J. Mougey, D. Royer, B. Saghai, D. Tarnowski, S. Turck-Chieze, M. Brussel, G.P. Capitani, E. De Sanctis, S. Frullani, F. Garibaldi, D.B. Isabelle, E. Jans, I. Sick, and P.D. Zimmerman. Deep-inelastic electron scattering from carbon. *Nuclear Physics A*, 402(3):515–540, 1983.

[48] J Benlliure. Isospin effects in fragmentation reactions. In *EPJ Web of Conferences*, volume 88, page 00028. EDP Sciences, 2015.

[49] Facility for Antiproton and Ion Research (FAIR).
https://www.gsi.de/en/researchaccelerators/fair.

[50] Institute of Physical and Chemical Research or Rikagaku Kenkyūsho.
https://www.riken.jp/en.

[51] Facility for Rare Isotope Beams (FRIB). https://frib.msu.edu.

[52] G.R. Satchler and W.G. Love. Folding model potentials from realistic interactions for heavy-ion scattering. *Physics Reports*, 55(3):183–254, 1979.

[53] L.C. Chamon, B.V. Carlson, and L.R. Gasques. São paulo potential version 2 (spp2) and brazilian nuclear potential (bnp). *Computer Physics Communications*, 267:108061, 2021.

[54] D. Chrisman, A. N. Kuchera, T. Baumann, A. Blake, B. A. Brown, J. Brown, C. Cochran, P. A. DeYoung, J. E. Finck, N. Frank, P. Guèye, H. Karrick, H. Liu, J. McDonaugh, T. Mix, B. Monteagudo, T. H. Redpath, W. F. Rogers, R. Seaton-Todd, A. Spyrou, K. Stiefel, M. Thoennessen, J. A. Tostevin, and D. Votaw. Neutron-unbound states in ^{31}Ne. *Phys. Rev. C*, 104:034313, Sep 2021.

[55] Dayah Chrisman. *Neutron-unbound states in the nucleus of ^{31}Ne.* PhD thesis, Michigan State University, 2022.

[56] P. Capel. private communication, 2023.

[57] The Modular Neutron Array (MoNA) Collaboation. https://www.monacollaboration.org.

[58] T. Redpath, T. Baumann, J. Brown, D. Chrisman, P.A. DeYoung, N. Frank, P. Guèye, A.N. Kuchera, H. Liu, C. Persch, S. Stephenson, K. Stiefel, M. Thoennessen, and D. Votaw. New segmented target for studies of neutron unbound systems. *Nuclear Instruments and Methods in Physics Research Section A: Accelerators, Spectrometers, Detectors and Associated Equipment*, 977:164284, 2020.

[59] M Nowakowski, E A Paschos, and J M Rodríguez. All electromagnetic form factors. *European Journal of Physics*, 26(4):545, apr 2005.

[60] D. Androić, D. S. Armstrong, J. Arvieux, S. L. Bailey, D. H. Beck, E. J. Beise, J. Benesch, F. Benmokhtar, L. Bimbot, J. Birchall, P. Bosted, H. Breuer, C. L. Capuano, Y.-C. Chao, A. Coppens, C. A. Davis, C. Ellis, G. Flores, G. Franklin, C. Furget, D. Gaskell, M. T. W. Gericke, J. Grames, G. Guillard, J. Hansknecht, T. Horn, M. Jones, P. M. King, W. Korsch, S. Kox, L. Lee, J. Liu, A. Lung, J. Mammei, J. W. Martin, R. D. McKeown, M. Mihovilovic, A. Micherdzinska, H. Mkrtchyan, M. Muether, S. A. Page, V. Papavassiliou, S. F. Pate, S. K. Phillips, P. Pillot, M. L. Pitt, M. Poelker, B. Quinn, W. D. Ramsay, J.-S. Real, J. Roche, P. Roos, J. Schaub, T. Seva, N. Simicevic, G. R. Smith, D. T. Spayde, M. Stutzman, R. Suleiman, V. Tadevosyan, W. T. H. van Oers, M. Versteegen, E. Voutier, W. Vulcan, S. P. Wells, S. E. Williamson, and S. A. Wood. Strange quark contributions to parity-violating asymmetries in the backward angle g0 electron scattering experiment. *Phys. Rev. Lett.*, 104:012001, Jan 2010.